Applied theory of bending vibration of the piezoelectric and piezomagnetic bimorph*

Do Thanh Binh[†], V. A. Chebanenko[‡], Le Van Duong[§], E. Kirillova[¶],
Pham Manh Thang[‖] and A. N. Soloviev[†,**,††]

[†]*Department of Theoretical and Applied Mechanics*
Don State Technical University
No. 1, Gagarin sq., Rostov-on-Don 344000, Russia

[‡]*Southern Scientific Center of RAS*
No. 41, Chekhov Avenue, Rostov-on-Don 344006, Russia

[§]*Department of Construction Machinery*
Le Quy Don Technical University
No. 236, Hoang Quoc Viet str., Hanoi 100000, Vietnam

[¶]*RheinMain University of Applied Sciences*
Kurt-Schumacher-Ring 18, Wiesbaden 65197, Germany

[‖]*Department of Engineering Mechanics and Automation*
Vietnam National University
No. 144, Xuan Thuy str., Hanoi 100000, Vietnam

[**]*Institute of Mathematics, Mechanics and Computer Sciences*
Southern Federal University, No. 8A, Milchakova St., Rostov-on-Don 344090, Russia
[††]solovievarc@gmail.com

Based on the variational principle, equations and boundary conditions for transverse steady vibrations of a bimorph consisting of a piezoelectric and piezomagnetic layers are obtained. The results of calculations of natural frequencies are compared with the finite element model of the device in ACELAN.

Keywords: Energy harvesting; piezoelectrics; piezomagnetics; applied theory.

1. Introduction

In the fabrication of sensor and measuring systems, modern small-sized household appliances, cellular telephones and wireless sensor systems for monitoring and diagnosing the technical condition of various objects, etc., powerful energy sources are not required, however, mobility and nonvolatility of the above devices are mandatory. Energy storage devices with piezoactive elements that directly convert the energy of mechanical vibrations into electrical energy are widely used to power such devices. In Refs. 1–3, energy storage devices using piezoelectric generators under the influence of mechanical loads were studied.

If the system is in an alternating magnetic field created by permanent magnets mounted on rotating parts of the machine, then in this case, the piezomagnetic layer is deformed together with the piezoelectric element, due to which an electric current is generated. In Refs. 7 and 8, Guo-Liang Yu *et al.* discussed the theoretical models of multilayer magnetoelectric composites for the magnetoelectric response at resonant frequencies corresponding to vibrations of the bending and extensional modes. A theoretical model of magnetic energy harvesters using functionally graded composites cantilever is analyzed to improve the harvesting ability and adjust the resonant frequency in Ref. 9. In Ref. 10, Zhanga *et al.* studied bifurcations, periodic and chaotic dynamics of a four-edged simply supported composite laminated piezoelectric rectangular plate. In Ref. 11, bending and free vibrations of a magnetoelectroelastic plate with surface effects were investigated.

In this paper, oscillations of the device are considered in the formulation of plane deformation. An applied theory of bending vibrations of a two-layer bimorph is constructed. Calculation results are compared with calculations using the finite element modeling in the ACELAN package.

---

2. Problem Formulation

General equations and defining relations for a piezo-magnetoelectric body consist of [4] the following:

$$\nabla \cdot \boldsymbol{\sigma} + \rho\mathbf{f} = \rho\ddot{\mathbf{u}}, \quad \nabla \cdot \mathbf{D} = \sigma_\Omega, \quad \nabla \cdot \mathbf{B} = 0. \quad (1)$$

$$\begin{aligned} \boldsymbol{\sigma} &= \mathbf{c} : \boldsymbol{\varepsilon} - \mathbf{e}^T \cdot \mathbf{E} - \mathbf{h}^T \cdot \mathbf{H} \\ \mathbf{D} &= \mathbf{e} : \boldsymbol{\varepsilon} + \kappa \cdot \mathbf{E} + \boldsymbol{\alpha} \cdot \mathbf{H} \quad , \\ \mathbf{B} &= \mathbf{h} : \boldsymbol{\varepsilon} + \boldsymbol{\alpha}^T \cdot \mathbf{E} + \boldsymbol{\mu} \cdot \mathbf{H}. \end{aligned} \quad (2)$$

$$\boldsymbol{\varepsilon} = \frac{1}{2}(\nabla\mathbf{u} + (\nabla\mathbf{u})^T), \quad \mathbf{E} = -\nabla\varphi, \quad \mathbf{B} = -\nabla\phi. \quad (3)$$

Here, $\boldsymbol{\sigma}$ denotes stress tensor, $\boldsymbol{\varepsilon}$ denotes strain tensor, $\mathbf{D}$ denotes electric displacement vector, $\mathbf{E}$ denotes electric field vector, $\mathbf{B}$ denotes magnetic induction vector, $\mathbf{H}$ denotes magnetic field vector, ρ denotes material density, $\mathbf{c}$ denotes elastic coefficients tensor, $\mathbf{e}$ denotes piezoelectric coefficients tensor, $\mathbf{h}$ denotes piezomagnetic coefficients tensor, κ denotes dielectric permittivity tensor, $\boldsymbol{\alpha}$ denotes magnetoelectric permeability tensor, $\boldsymbol{\mu}$ denotes magnetic permeability tensor, $\mathbf{f}$ denotes mass forces density vector, σ_Ω denotes volume density of electric charges, $\mathbf{u}$ denotes displacement vector, φ and ϕ denote electric and magnetic potentials, respectively.

The boundary conditions are determined for the mechanical, electric, and magnetic fields, respectively.

The mechanical conditions are formulated as follows. Suppose that surface S consists of two parts Γ_1 and Γ_2, so that $S = \Gamma_1 \cup \Gamma_2$, and $\Gamma_1 \cap \Gamma_2 = \varnothing$.

$$\mathbf{u} = \mathbf{U} \text{ on } \Gamma_1, \quad \mathbf{n} \cdot \boldsymbol{\sigma} = \mathbf{p} \text{ on } \Gamma_2. \quad (4)$$

Next, the electric conditions are formulated as follows. Suppose that surface S consists of two parts Γ_3 and Γ_4, so that $S = \Gamma_3 \cup \Gamma_4$, and $\Gamma_3 \cap \Gamma_4 = \varnothing$.

$$\varphi = \varphi(\mathbf{x}, t) \text{ on } \Gamma_3, \quad \mathbf{n} \cdot \mathbf{D} = -\sigma_0 \text{ on } \Gamma_4. \quad (5)$$

Here, σ_0 denotes density of surface charges. In addition, if the electrodes are connected to an external circuit, two conditions must be added

$$\varphi|_{S_E} = v, \quad \int\int_{S_E} \mathbf{n} \cdot \mathbf{D}\,dS = I. \quad (6)$$

Here, S_E denotes area of electrode, v denotes unknown potential, which is found from the second condition and I denotes electric current.

In the end, the magnetic conditions are formulated as follows. Suppose that surface S consists of two parts Γ_5 and Γ_6, so that $S = \Gamma_5 \cup \Gamma_6$, and $\Gamma_5 \cap \Gamma_6 = \varnothing$.

$$\phi = \phi(\mathbf{x}, t) \text{ on } \Gamma_5, \quad \mathbf{n} \cdot \mathbf{B} = \sigma_1 \text{ on } \Gamma_6. \quad (7)$$

Here, σ_1 denotes density of surface free currents along the boundary.

The components of the displacement vector $\mathbf{u}$ of the elastic layer of the substrate are unknown, the electric potential φ is added to the piezoelectric layer, and the magnetic potential ϕ is added to the piezomagnetic layer, in this case,

relations (2) are transformed by equating the corresponding constants to zero.

3. Finite Element Modeling

In the finite element package, ACELAN, a model of a piezomagnetoelectric energy storage device, was built based on two plates. Piezoelements (PE) consist of one piezoelectric and one piezomagnetic plate polarized by thickness H_1 and H_2, respectively. The problem is considered in the statement of plane deformation, the device consists of two rectangles, the dimensions of which are given as follows.

The finite element model of the device was built in the ACELAN software, where piezoelectric layers were modeled by six-node triangular finite element. In this work, the piezomagnetic layer can also be modeled by the same finite element, in which the piezoelectric material properties are replaced by piezomagnetic. This can be accomplished for reasons: qualitatively, the equations for the electric and magnetic potentials coincide.

Tables 1 and 2 present constants of piezoelectric and piezomagnetic layers, which are used in calculations: piezoelectric-PZT-4, piezomagnetic-CoFe$_2$O$_4$.[5,6]

Here, C_{ij}^E (GPa) denotes elastic coefficients, e_{ij} (C/m^2) denotes piezoelectric coefficients, k_{ij} and ε_0 denote dielectric permittivity, $\varepsilon_0 = 8,85 \times 10^{-12}$ F/m, density of piezoceramics PZT-4: $\rho = 7500$ kg/m^3.

Here, C_{ij}^M (GPa) denotes elastic coefficients, Q_{ij} (N/A m) denotes piezomagnetic coefficients, λ_{ij} (10^{-6} N s^2/C^2) — magnetic permeability, density of piezomagnetic element CoFe$_2$O$_4$: $\rho = 5290$ kg/m^3.

Figure 1 shows the distribution of horizontal displacements (Fig. 1(a)), vertical displacements (Fig. 1(b)), electric and magnetic potentials (Fig. 1(c)), longitudinal strain

Table 1. Material properties of piezoceramics PZT-4.

C_{11}^E	C_{12}^E	C_{13}^E	C_{33}^E	C_{44}^E
139	77.8	74.3	115	25.6
e_{31}	e_{33}	e_{15}	k_{11}/ε_0	k_{33}/ε_0
−5.2	15.1	12.7	730	635

Table 2. Material properties of piezomagnetic element CoFe$_2$O$_4$.

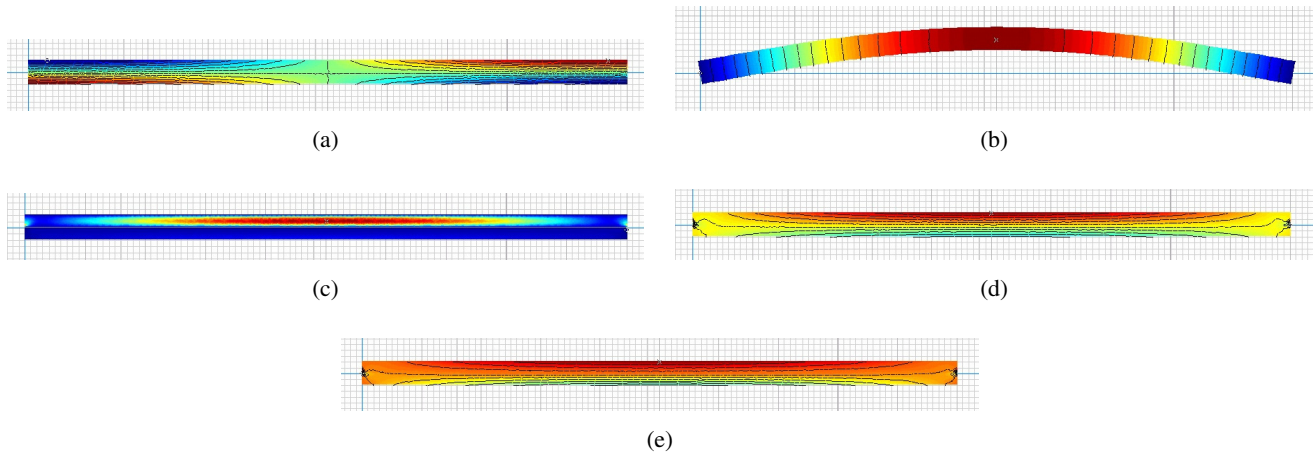| C_{11}^M	C_{12}^M	C_{13}^M	C_{33}^M	C_{44}^M
286	173	170	269.5	45.3
Q_{31}	Q_{33}	Q_{15}	λ_{11}	λ_{33}
580.3	699.7	550	590	157

Fig. 1. Distribution of: (a) horizontal displacements, (b) vertical displacements, (c) electric and magnetic potentials, (d) longitudinal strain and (e) longitudinal stress.
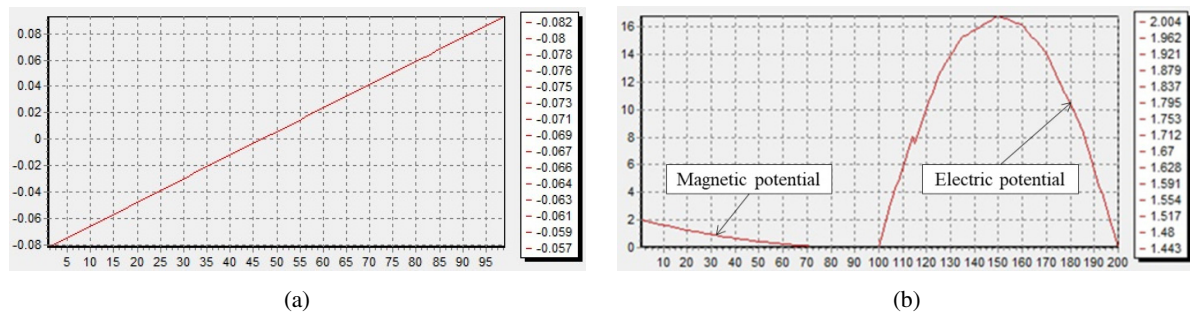

Fig. 2. Distribution of: (a) horizontal displacements, (b) electric and magnetic potentials along the thickness of the bimorph.

(Fig. 1(d)), longitudinal stresses (Fig. 1(e)) at the frequency of the first resonance (first bending mode). The thickness of the layers is 0.2 mm, the length of the bimorph is 10 mm. The bimorph is pinned at the ends, the upper and lower surfaces of the piezoelectric element are electroded, and the magnetic potential is set to zero on the inner surface of the piezo-magnetic layer.

Figure 2 shows the distribution of horizontal displace-ments (Fig. 2(a)), electric and magnetic potentials along the thickness of the bimorph (Fig. 2(b)) at the frequency of the first resonance. It should be noted that the abscissa axis in Figs. 2 and 3 corresponds to the numbers of the points at which measurements were made. An analysis of Figs. 1 and 2 shows that the distribution of the longitudinal displacement is linear, the distribution of the transverse displacement along the thickness is constant, accurately describing the deformed state of the bimorph. The distribution of the electric potential can be assumed to be quadratic in range from 100 to 200 in Fig. 2(b). The distribution of the magnetic potential is linear in the range from 0 to 100 in Fig. 2(b).

It should be noted that for a bimorph with the same thickness of the piezoelectric and piezomagnetic layers, the neutral line for longitudinal displacements runs slightly below their interface region (the intersection of the dotted

zero line and graph in Fig. 2(b) is moved to the left of the number 50 — the middle of the layer), which is explained by a significant difference in the elastic properties of these materials (Tables 1 and 2).

Figure 3 shows the distribution of horizontal displacement of a bimorph with layer thickness ratio 2:3 (piezomagnetic — 0.2 mm and piezoelectric — 0.3 mm, respectively). The graph that intersects with dotted zero line at the point has an abscissa of 100, which corresponds to the interface boundary i.e., with this thickness ratio of the layers, the device works most efficiently because longitudinal displacements and strains have the same signs within each piezoactive layer and are different in different layers.
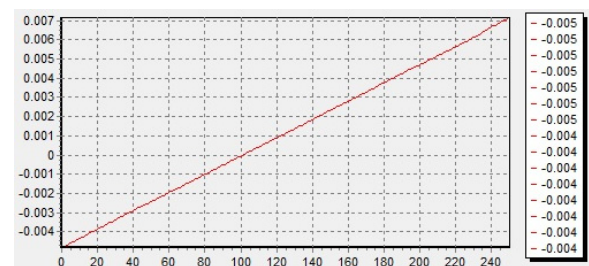

Fig. 3. Distribution of horizontal displacements along thickness.

4. Applied Theory

In this work, based on the variational principle and Kirchhoff–Love hypotheses for the transverse bending of plates on the distribution of mechanical, electric and magnetic fields, a system of equations describing the cylindrical bimorph bending is obtained. The general form of the variational equation for the case of steady-state oscillations with a frequency ω of a flat body with an area S has the following form:

$$\iint_S \delta\tilde{H}dS - \rho\omega^2 \iint_S u_i\delta u_i dS$$
$$+ \iint_S (p_i\delta u_i + \sigma_0\delta\varphi + \sigma_1\delta\phi)dS = 0. \quad (8)$$

Here, $\delta\tilde{H} = \sigma_{ij}\delta\varepsilon_{ij} - D_i\delta E_i - B_i\delta H_i$ denotes enthalpy variation and indices i and j take values of 1, 3.

In particular, the hypothesis of a single normal is accepted for a mechanical field, since a problem in which there is a difference in electric potential on the electrodes (it is equal to zero on one electrode, on other electrode, the output voltage is defined by Eq. (6)) is considered. Its distribution at the first modes of oscillations is described quite accurately by a linear function, but takes into account the possible heterogeneity along the length of the element associated with the influence of boundary conditions at the ends of the bimorph. Then its distribution is taken as a quadratic function, the magnetic potential at the inner boundary of the piezomagnetic layer is taken as zero, at the outer boundary the distribution σ_1 is uniform, so the magnetic potential distribution is assumed to be linear and nonuniform along the length of the element. Thus, the problem takes the form of a system of ordinary differential equations for the deflection of the plate $u_3 = w(x, \omega)$ and the distribution functions of the electric and magnetic potentials in the middle of the piezoelectric $\Phi(x)$ and at the outer boundary of the piezomagnetic layer $\Xi(x)$.

The result is a system of three differential equations as follows:

$$\frac{2e_{31}H_1}{3}\left(\frac{d^2}{dx^2}\Phi(x)\right)$$
$$+ \frac{(H_1^3 c_{p11} + H_2^3 c_{m11})}{3}\left(\frac{d^4}{dx^4}w(x)\right)$$
$$+ \frac{\omega^2(H_1^3\rho_p + H_2^3\rho_m)}{3}\left(\frac{d^2}{dx^2}w(x)\right)$$
$$- \omega^2(H_1\rho_p + H_2\rho_m)w(x)$$
$$- p_1(x) - p_2(x) - \frac{h_{31}H_2}{2}\left(\frac{d^2}{dx^2}\Xi(x)\right) = 0, \quad (9)$$

$$\frac{8\varepsilon_{11}H_1}{15}\left(\frac{d^2}{dx^2}\Phi(x)\right) + \frac{8\varepsilon_{33}V_1}{3H_1} - \frac{16\varepsilon_{33}\Phi(x)}{3H_1}$$
$$+ \frac{8\varepsilon_{33}V_3}{3H_1} + \frac{2H_1e_{31}}{3}\left(\frac{d^2}{dx^2}w(x)\right) = 0, \quad (10)$$

$$\frac{\mu_{11}H_2}{3}\left(\frac{d^2}{dx^2}\Xi(x)\right) - \frac{h_{31}H_2}{2}\left(\frac{d^2}{dx^2}w(x)\right)$$
$$+ \frac{\mu_{33}(M_1 - \Xi(x))}{H_2} = 0. \quad (11)$$

To satisfy the boundary conditions at the ends of the bimorph, expressions for the transverse force (Eq. (12)), bending moment (Eq. (13)), and the components of the electric displacement (Eq. (14)) and magnetic induction (Eq. (15)) vector are obtained, respectively.

$$Q_x = -\frac{2e_{31}H_1}{3}\left(\frac{d}{dx}\Phi(x)\right)$$
$$- \frac{(H_1^3 c_{p11} + H_2^3 c_{m11})}{3}\left(\frac{d^3}{dx^3}w(x)\right)$$
$$- \frac{\omega^2(H_1^3\rho_p + H_2^3\rho_m)}{3}\left(\frac{d}{dx}w(x)\right)$$
$$+ \frac{h_{31}H_2}{2}\left(\frac{d}{dx}\Xi(x)\right). \quad (12)$$

$$M_x = \frac{e_{31}H_1V_1}{6} - \frac{5e_{31}H_1V_3}{6} + \frac{2e_{31}H_1\Phi(x)}{3}$$
$$+ \frac{H_1^3 c_{p11} + H_2^3 c_{m11}}{3}\left(\frac{d^2}{dx^2}w(x)\right)$$
$$+ \frac{h_{31}H_2(M_1 - \Xi(x))}{2}, \quad (13)$$

$$D_1 = -\frac{8\varepsilon_{11}H_1}{15}\left(\frac{d}{dx}\Phi(x)\right), \quad (14)$$

$$B_1 = -\frac{\mu_{11}H_2}{3}\left(\frac{d}{dx}\Xi(x)\right). \quad (15)$$

The results of the numerical calculations according to the proposed applied theory were compared with the calculation performed using the FEM in ACELAN. Table 3 presents the errors in finding the maximum deflection, electric and magnetic potentials for oscillations at frequency of 100 Hz, with uniformly distributed mechanical load of 1000 Pa, for different thickness ratios of the piezomagnetic and piezoelectric layers.

Table 3 presents the comparison results of errors in finding the maximum deflection, the electric and magnetic potentials. These results show that when the thickness ratio corresponds

Table 3. Comparison of of errors in finding the maximum deflection, the electric and magnetic potentials.

Thickness of the piezomagnetic and piezoelectric layers, respectively (mm)	0.2	0.2–0.4	0.2–0.3
Deflection (%)	2.6	3.7	0.7
Electric potential (%)	1.8	3.4	0.07
Magnetic potential (%)	10	8	2.4
The first resonant frequency (%)	1.3	1.5	0.3

to the position of the neutral line at the interface boundary, the applied theory adequately describes the mechanical, electric and magnetic fields in the bimorph. So, the error in finding the first resonant frequency of 10.067 kHz for the case of 0.2:0.3 (column 4 of Table 3) is less than 1%.

5. Conclusion

An applied theory is proposed for calculating the transverse vibrations of a bimorph consisting of two layers: piezoelectric and piezomagnetic. In the piezoelectric layer, the quadratic distribution of the electric potential along the thickness is assumed, in the piezomagnetic layer, the linear distribution of the magnetic potential is assumed. A comparison of the calculation results of the device in the low-frequency region (the first resonant frequency of bending vibrations) is made, which showed that the error in finding the characteristics of the mechanical and electric fields, as well as the resonant frequency, is less than 1%.

Acknowledgments

References

[1] S. N. Shevtsov, A. N. Soloviev, I. A. Parinov, A. V. Cherpakov and V. A. Chebanenko, *Piezoelectric Actuators and Generators for Energy Harvesting*, (Springer, Heidelberg, 2018).

[2] V. D. Le, Finite-element modeling of piezoelectric energy storage devices with complicated physical and mechanical properties, for the degree of PhD dissertation, Don State Technical University, Russia (2014).

[3] V. D. Le, M. T. Pham, V. A. Chebanenko, A. N. Soloviev and C. V. Nguyen, Finite element modeling and experimental studies of stack-type piezoelectric energy harvester, *Int. J. Appl. Mech* **9**(6), 1750084 (2017).

[4] N. V. Kurbatova, D. K. Nadolin, A. V. Nasedkin, P. A. Oganesyan and A. N. Soloviev, Finite element approach for composite magneto-piezoelectric materials modeling in ACELAN-COMPOS package, *Analysis and Modelling of Advanced Structures and Smart Systems.* Series "Advanced Structured Materials", Vol. 81, eds. H. Altenbach, E. Carrera and G. Kulikov, Chapter 5 (Springer, Singapore, 2018), pp. 69–88.

[5] J.-Y. Kim, Micromechanical analysis of effective properties of magneto-electro-thermo-elastic multilayer composites, *Int. J. Eng. Sci.* **49**(9), 1001 (2011).

[6] K. S. Challagulla and A. V. Georgiades, Micromechanical analysis of magneto-electro-thermo-elastic composite materials with applications to multilayered structures, *Int. J. Eng. Sci.* **49**(1), 85 (2011).

[7] G.-L. Yu, H.-W. Zhang, F.-M. Bai, Y.-X. Li and J. Li, Theoretical investigation of magnetoelectric effect in multilayer magneto-electric composites, *Compos. Struct. J.* **119**, 738 (2015).

[8] G.-L. Yu, H.-W. Zhang, Y.-X. Li and J. Li, Equivalent circuit method for resonant analysis of multilayer piezoelectric-magnetostrictive composite cantilever structures, *Compos. Struct. J.* **125**, 467 (2015).

[9] Y. Shi, H. Yao and Y.-W. Gao, A functionally graded composite cantilever to harvest energy from magnetic field, *J. Alloys Compds.* **693**, 989 (2017).

[10] Y. F. Zhanga, W. Zhangb and Z. G. Yao, Analysis on nonlinear vibrations near internal resonances of a composite laminated piezoelectric rectangular plate, *Eng. Struct. J.* **173**, 89 (2018).

[11] Y. Yang and X.-F. Li, Bending and free vibration of a circular magnetoelectroelastic plate with surface effects, *Int. J. Mech. Sci.* **157**, 858 (2019).